CHAPTER 24

EFFECT OF BOUSSINESQ EQUATIONS ON WAVE SPECTRA PROPAGATION

J.P.Sierra, A.S.Arcilla*, J.J.Egozcue**and J.L.Monso**

ABSTRACT

A 2-D numerical model has been developed to simulate wave propagation prior to breaking. This non linear hydrodynamic model works in connection with various spectral analysis routines. This paper intends to study the propagation effects on the wave time-series and on the corresponding spectral density functions in order to gain insight on both the spectral description of waves and irregular wave propagation.

1.- INTRODUCTION

Flow properties in coastal areas are of great importance in Maritime Engineering, for the solution of numerous problems such as the desing of offshore and coastal structures, shore evolution analysis, ship motions etc. For all of these subjects, a detailed konwledge of the shallow water wave heigth and propagation direction are required. State of art wave propagation models are usually either linear or unidirectional (in the input).

However, in order to enable the characterizacion of desing wave conditions, the use of two parameters as wave height and period is not enough. Wave randomness must be considered, since the assumption of unidirectional and monochromatic waves, can lead to unnacceptable results from the Maritime Engineering standpoint.

One of the best ways to describe the wave irregularity is through a spectral density function, which is able to condense easily all the information involved in a wave time-series, with different frequencies and wave heights. If the possibility of waves travelling in different directions is considered, the estimation of the directional spectrum will be necessary, in order to achieve a full description of the wave characteristics.

Although spectral analysis has been widely used for several decades, a non linear model has been seldom coupled with spectral models.

In this paper a 2-D numerical non linear model for the simulation of wave propagation prior to breaking is described. In this model, both regular and irregular wave trains can be used. The propagation effects on the wave time-series and on the spectral density function are studied, in order to gain insigth on both the spectral description of waves and irregular wave propagation.

* Maritime Eng.Lab., Catalonia University of Techn. in Barcelona. Spain.
** Department of Numerical Methods., Catalonia Univ. of Techn. in Barcelona.

2.- WAVE PROPAGATION

The numerical model is based on Boussinesq-type equations, in which the vertical velocity of the fluid particles is supposed to increase linearly from zero at the bed to a maximum magnitude at the free surface. The Boussinesq equations are formulated in terms of vertically-integrated mass and momentum conservation laws and are obtained with a perturbation tecnique (S.Arcilla and Monso, 1985), yielding the following expressions (Peregrine, 1967).

- Continuity equation

$$\frac{\partial H}{\partial t} + \frac{\partial p}{\partial x} + \frac{\partial q}{\partial y} = 0 \tag{1}$$

- x-momentum equation

$$\frac{\partial p}{\partial t} + \frac{\partial}{\partial x}\left(\frac{p^2}{H}\right) + \frac{\partial}{\partial y}\left(\frac{p.q}{H}\right) + gH\frac{\partial(H-h)}{\partial x} =$$

$$\frac{Hh}{2}\left[\frac{\partial^3(\frac{hp}{H})}{\partial t\partial x^2} + \frac{\partial^3(\frac{hq}{H})}{\partial t\partial x\partial y}\right] - \frac{h^2H}{6}\left[\frac{\partial^3(\frac{p}{H})}{\partial t\partial x^2} + \frac{\partial^3(\frac{q}{H})}{\partial t\partial x\partial y}\right] \tag{2}$$

-y-momentum equation

$$\frac{\partial q}{\partial t} + \frac{\partial}{\partial x}\left(\frac{p.q}{H}\right) + \frac{\partial}{\partial y}\left(\frac{q^2}{H}\right) + gH\frac{\partial(H-h)}{\partial y} =$$

$$\frac{Hh}{2}\left[\frac{\partial^3(\frac{hp}{H})}{\partial t\partial x\partial y} + \frac{\partial^3(\frac{hq}{H})}{\partial t\partial y^2}\right] - \frac{h^2H}{6}\left[\frac{\partial^3(\frac{p}{H})}{\partial t\partial x\partial y} + \frac{\partial^3(\frac{q}{H})}{\partial t\partial y^2}\right] \tag{3}$$

Where $H = h + \eta$

h is the still water depth

η is the free surface elevation

$p = \int_{-h}^{\eta} u.dz$ is the mass flux along the x axe.

$q = \int_{-h}^{\eta} v.dz$ is the mass flux along the y axe

u,v are the particle velocities along the x,y, axes.

Other terms can be easily included in these momentum equations, (S.Arcilla and Monso, 1986). With these additional terms, (e.g.Coriolis acceleration, wind friction, turbulent viscosity or bottom friction) a large number of physical phenomena can be adequately reproduced by the model.

The momentum conservation laws are highly non linear differential equations, and they include a third order derivative term, which is due to the existence of a constant vertical acceleration.

The vertical integration of equations (1),(2) and (3) reduces the problem from three to two indepedent dimensions. These equations are suitable for a wide range

of wave lenghts. In particular, short wind waves in shallow water provide an acceptable ratio of water depth to wave length except for the shortest waves. These waves can be thus considered as long waves, and their propagation can be correctly simulated by the model.

The behaviour of different kinds of waves can be characterized by Ursell's parameter (UR).

$$UR = \eta \frac{L^2}{h^3} \tag{4}$$

Boussinesq equations ($UR = O(1)$) degenerate into de linear long-wave equations ($UR << 1$) or the Airy equations ($UR >> 1$) with certain additional errors (S. Arcilla et al.,1985). This means that a single model, based on Boussinesq-type equations may be used to cover the whole range of physical problems (provided the associated errors are acceptable). When waves are of finite amplitude, the ratio h/L is small and breaking does not occur.

Considering different terms of the momentum equations and varying initial and boundary conditions, it is possible to reproduce a wide variety of physical phenomena such as Kelvin waves, storm surges, solitary waves, refraction, reflexion, diffraction, bottom friction, etc.

The equations are solved by means of an implicit centered finite-differences technique with variables defined on a space staggered rectangular grid. A double-sweep algorithm (Abbott and Ionescu, 1967) is invoked for solving the system avoiding large and expensive matrix inversion operations.

The truncation errors are of second order in time and space, i.e. $T.E. = O(\Delta x^2, \Delta y^2, \Delta t^2)$. The numerical scheme is conditionally stable and convergent. The propagation model is valid and yields reasonable results when $h/L < 0.2$. This means that the model can be applied in shallow or intermediate water depth but not in deep water.

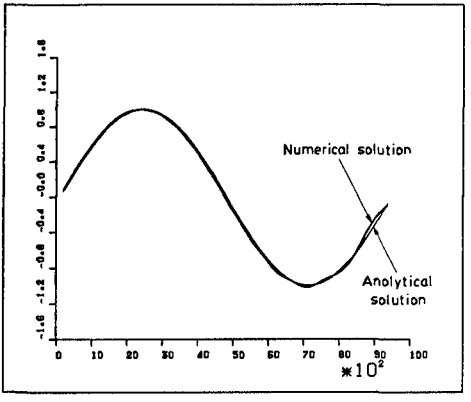

Figure 1. Sinusoidal long wave propagation

In open boundaries, an absorbing-reflecting boundary condition (S. Arcilla et al., 1986) is used. In this way, the multiple reflections due to innerly reflected waves are avoided, because these reflected waves are allowed to escape the domain unhampered.

The model was first calibrated in its linear version. Here, the momentum equations only include the local acceleration and the linear part of the pressure gradient term.

Figure 1 shows the application of the model for a sinusoidal long wave propagation. The characteristics of the discretization were $\Delta x = 200\ m.$, $\Delta y = 200\ m.$ and $\Delta t = 5\ s.$

The wave parameters were : Wave amplitude a=1 m., wave period T=300 s., wave length L=9389 m. and the depth was h=100 m.

The figure shows a good agreement between the numerical model results and the analytical solution.

Another test was made for sinusoidal short waves in shallow water. The characteristics of the discretization were $\Delta x = 3\ m.$, $\Delta y = 3\ m.$ and $\Delta t = 1\ s.$

and the wave parameters were Wave amplitude a=1 m., wave period T=18 s., wave length L=125 m. in a depth of h=5 m.

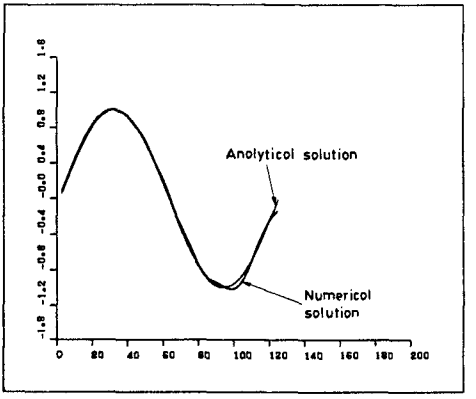

Figure 2. Sinusoidal short wave in shallow water propagation

Figure 2 shows that as the wave progresses the quality of the results decreases, although the fit between numerical and theoretical solutions is relatively acceptable. The poor quality of the results is obviously due to the fact that linear theory is not valid in shallow water.

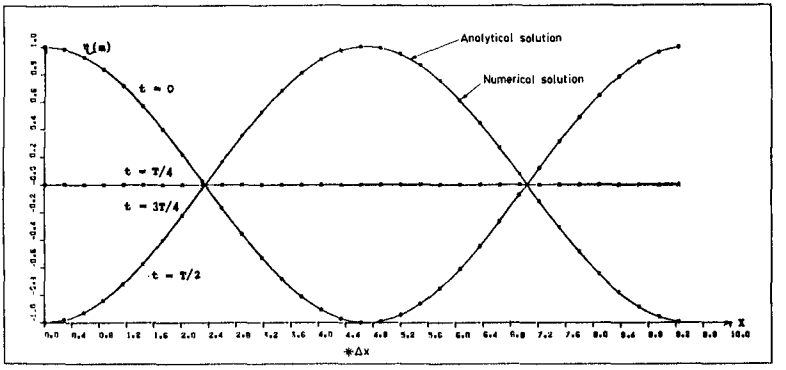

Figure 3. Reflection of a sinusoidal wave

Once the model had been tested for wave propagation, tests were made for reflecting waves, comparing computed results with the theoretical solution. Figure 3 shows the reflection of a sinusoidal wave on a vertical wall with constant water depth, forming a stationary wave.

The discretization and wave characteristics are the same as in the example showed in figure 1. The fit at different instants of time, between numerical and analytical results is excellent.

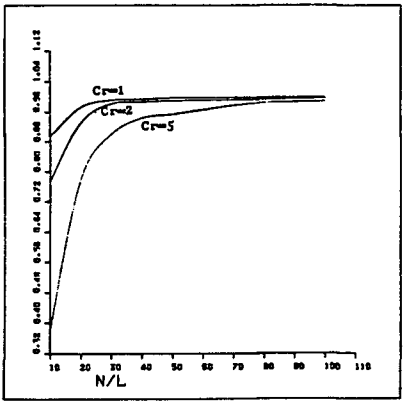

Figure 4. Illustration of model accuracy for different Courant numbers

Finally, phase and amplitude portrait errors were analysed. As an example, figure 4 shows the ratio of numerical celerity to theoretical celerity vs the number of points per wave length for different Courant numbers. It is seen that, for Cr=1, an acceptable accuracy is obtained with values of $N/L > 20$. When the Courant number increases, it is difficult to get a similar accuracy though more points per wave length are used.

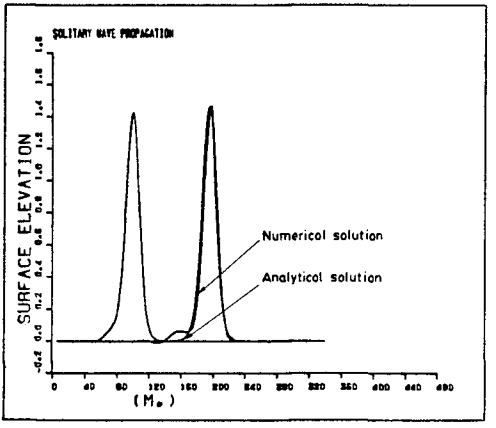

Figure 5. Solitary wave propagation

After the linear version was calibrated, the non linear model was tested with cnoidal wave theoretical solutions, using equations (1), (2) and (3). The analytical solution of these equations, that exclude frictional stresses, Coriolis accelerations and similar terms, is the solitary wave. Figure 5 demostrates the good fit between

numerical and theoretical results after 24 seconds. The discretization characteristics were $\Delta x = 2.5\ m.$, $\Delta y = 2.5\ m.$ and $\Delta t = 0.25\ s.$

and the wave parameters were wave height $H_0 = 1.5\ m.$, depth $h = 5\ m.$

3.- SPECTRAL MODELS

In scalar spectral analysis, numerous models exist for time series generation and processing. These models are based on different techniques and may be divided in two groups:

- Conventional methods, based on the Fast Fourier Transform (FFT) algorithm (Cooley and Tukey, 1965).

-Parametric methods, involving autoregresive (AR) and autoregresive-moving average (ARMA) models.

Every technique presents several advantages and inconvenients with respect to the others. Therefore, the selection in every case of the most suitable algorithm will be necessary. For improving the use of design spectra in Maritime Engineering, several pattern spectra have been introduced in last decades. These spectra depend on various parameters. Fitting the parameters to the local conditions, a representative spectrum is obtained. The Pierson-Moskowitz spectrum (Pierson and Moskowitz, 1964) and the JONSWAP spectrum (Hasselman et al.,1973) are the most well-known ones. However, the two formulations are only accepted in deep water. In shallow water, the use of suitable spectra as TMA spectrum (Bouws et al.,1983) is needed.

An example of the use of scalar spectral analysis techniques, in which the time series is generated from a JONSWAP spectrum through an ARMA(8,1) model, is showed in figure 6. The parameters of the JONSWAP spectrum were $\sigma_a = 0.07$, $\sigma_b = 0.09$, $\alpha = 0.03$, $\gamma = 3.3$ and $\omega_m = 0.18$

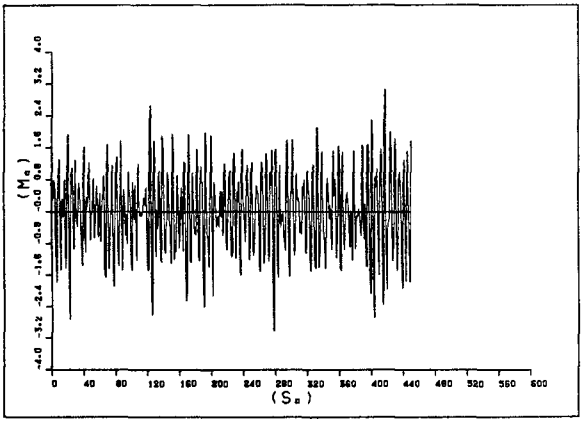

Figure 6. Time series generated from a JONSWAP spectrum

In figure 7, three spectra are plotted. They belong to the initial JONSWAP spectrum, the theoretical spectrum calculated from the autocorrelation function corresponding the JONSWAP, and the spectrum evaluated from the time series simulated. The agreement between the three spectra is remarkable, showing the validity of the time series generation technique.

On the other hand, the determination of the directional spectral density function $S(\omega,\theta)$ is made by recasting the function as

$$S(\omega,\theta) = S(\omega).D(\omega,\theta) \tag{5}$$

with

$$\int_0^{2\pi} D(\omega,\theta).d\theta = 1 \tag{6}$$

where $S(\omega)$ is the scalar spectral density function, computed using one of the aforementioned methods, and $D(\omega,\theta)$ is the directional spreading function. A convenient approximation to this function may be obtained by expanding $D(\omega,\theta)$ as a Fourier series as

$$D(\omega,\theta) = \frac{1}{\pi}\left[\frac{1}{2} + \sum_{n=1}^{\infty}(a_k.cosk\theta + b_k.sink\theta)\right] \tag{7}$$

a_k, b_k are Fourier coefficients

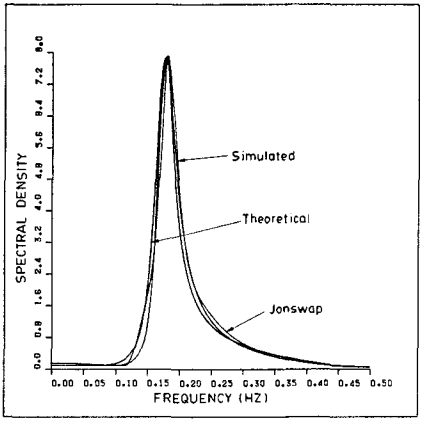

Figure 7. Spectral density functions of the time series generated

Measurement of directional waves in Nature are rather difficult. For this purpose, the pitch-roll buoy is one of the most extended instruments nowadays. This device provides three time series corresponding to the free surface elevation $\eta(t)$, and the wave slopes in two perpendicular directions $\eta_x(t)$, $\eta_y(t)$. Having time series of three canals, just the two first Fourier coefficients can be computed only.

For the estimate of the directional spectrum, the way to be followed involves three steps :

i) Determination of the cross spectra between the time series

ii) Computation of the Fourier coefficients for different frecuencies.

iii) Interpolation of the directional spectrum. This last step may be carried out by two ways. The first is fitting the directional spectrum to prefixed distribution functions. The second is the rational interpolation through AR and ARMA models. The latter was tested with 10 directional wave records obtained in the North Sea the 1-12-1983 and provided by the Programa de Clima Marítimo of the Ministry of Public Works (MOPU) in Spain. These time series were recorded at intervals

of 3 hours on a well developed sea with a wind direction of $250 - 260^0$ for the first series. The wind direction changes to 0^0 in the tenth series, producing a change in the wave direction for the high frequencies.

Figures 8 and 9 show the wind and wave mean direction for the first and the tenth records.

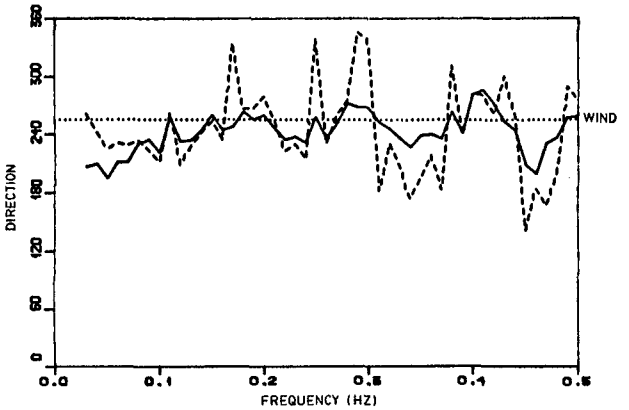

Figure 8. Wind and wave mean direction. Series 1

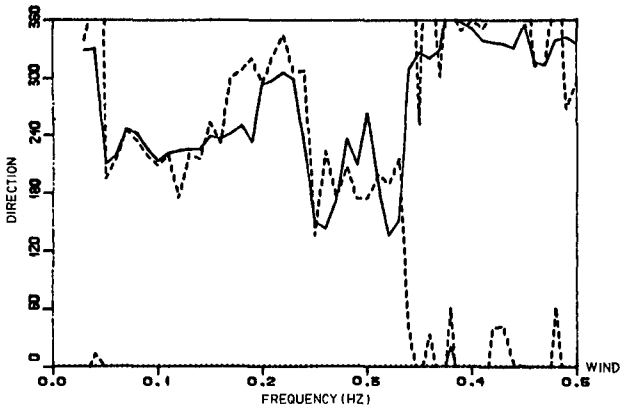

Figure 9. Wind and wave mean direction. Series 10

The directional spectra from these records (with three time series $\eta(t)$, $\eta_x(t)$, $\eta_y(t)$ in every record), were determined using rational interpolation through AR and ARMA models. In figures 10 and 11, the directional spectrum modes, i.e. the predominant directions, for every frequency are plotted. The results show a good reproduction of the mean direction in the directional spectra calculated.

The use of rational interpolation gives an aditional advantage, since it is very easy to reverse the procedure and given a directional spectrum to generate a record. This record will be composed of three time series corresponding to the free surface elevation $\eta(t)$ and other two parameters, such as the wave slopes $\eta_x(t)$, $\eta_y(t)$. Nevertheless, these two parameters may be replaced for others if the transference function is changed.

4.- WAVE TIME-SERIES PROPAGATION

As it has been showed in section 2, the present model reproduces closely the different phenomena involved in the regular wave trains propagation. In the case of irregular waves, it would be necessary to determine each parameter from the field data or calibrate them with physical models. Both possibilities, are out of the scope of this work. Because of the difficulty of handling large wave records, the authors have assumed their representation by means of the spectral density function. Therefore, when random waves are used, the calibration of the model is done assuming the invariability of the spectrum when waves travel on a constant deep area and without obstacles that could interfere their propagation.

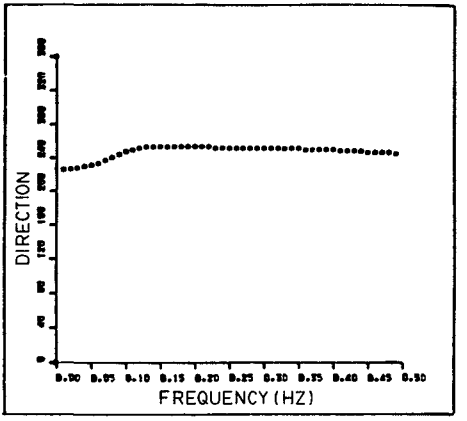

Figure 10. Predominant directions in directional spectrum. Series 1

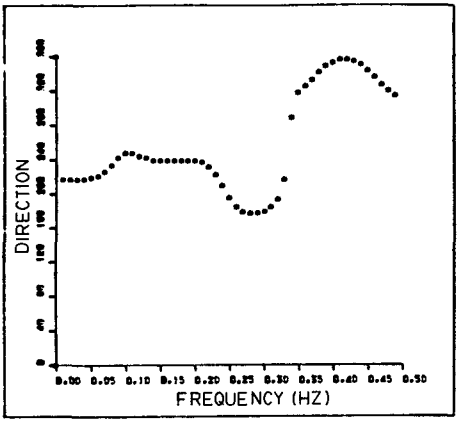

Figure 11. Predominant directions in directional spectrum. Series 10

A time series generated by means of one of the aforementioned techniques was propagated using the Boussinesq model, over a fluid domain with horizontal bottom and with a depth of 5 m. The result was another time series. As the visual comparison between the two time series is very difficult, their characteristics have been confronted computing the spectral density functions, that are showed in figure 12. The plots of these functions are practically identical and therefore it implies that the numerical model reproduces accurately the irregular wave propagation, over a horizontal bottom.

Another case analysed was the refraction of irregular wave over an uniform slope. Figure 13 presents the spectral density functions of the time series before and after the refraction. In this plot it is shown that the peak period is the same, but refraction produces a secondary peak with a frequency that is nearly twice the peak frequency. Then refraction produces a transference of energy towards higher frequencies, keeping the peak period but decreasing the mean period.

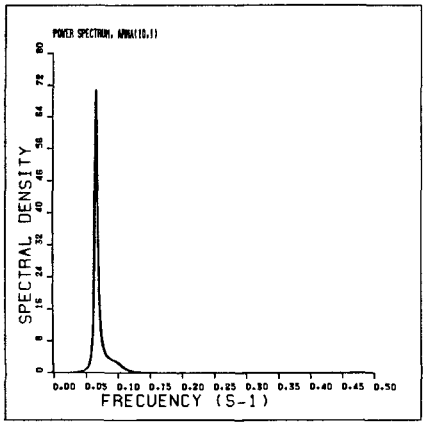

Figure 12. Spectra of the generated and propagated time series

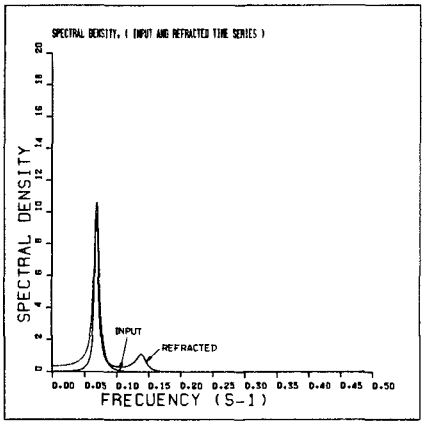

Figure 13. Spectral density functions of the initial and refracted time series

Moreover the study of the difraction of irregular waves was carried out. In this study, a linearized version of the numerical model was employed. In figure 14, the fluid domain is illustrated. The boundary with the gap is a vertical wall. The other boundaries are open, to avoid reflections. In the points A,B,C, and D, the free surface elevation was recorded. When the time series were obtained, the spectral density functions were determined and compared with the spectral density function of the initial time series, as it is showed in figure 15. The analysis of these figures shows logical results because the greater the distance to the gap is, the smaller the area comprised below $S(\omega)$ is, i.e. the energy of the spectrum decreases when the point is far away. On the other hand, the peak frequency does not change after difraction in all points inside the fluid domain, though this circumstance can be due to the use of a lynearized version of the propagation model.

Finally, a real example has been analysed. Here, the lay-out and the bathymetry are the ones corresponding to a Spanish harbour. Figure 16a represents the input wave spectrum used at the entrance of the harbour. This spectrum has been derived from field measurements.

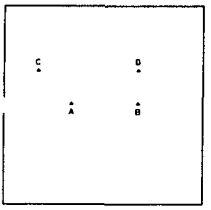

Figure 14.Difraction study. Fluid domain.

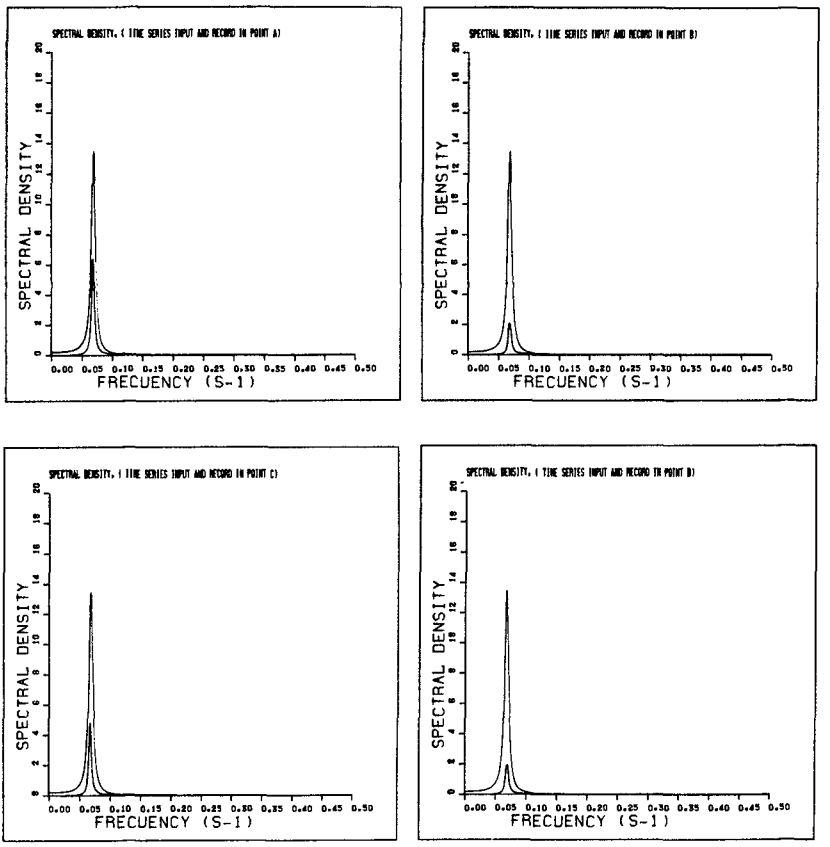

Figure 15. Spectral density function before and after difraction.

Figure 16b shows the result of carrying out an ARMA spectral process of the surface elevation time series, obtained after a run of the propagation model, inside a basin of the harbour. This output wave spectrum has a secondary peak in the origin. Since the spectrum has been plotted with 100 points, the secondary peak means that a long wave with a period up to 200 seconds is present in the time series recorded by the numerical model inside the basin. Actually similar wave conditions to those of the numerical simulation gave way to the record of long waves with a period of 240 seconds in the same basin. Therefore, the propagation model allows simulating and discovering long wave phenomena in real cases.

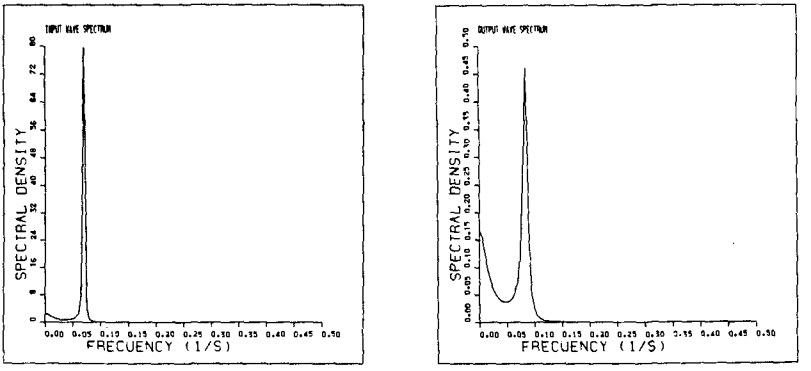

Figure 16. Input and output wave spectrum.

5. CONCLUSIONS AND FUTURE PERSPECTIVES

The main conclusions of this paper are

- The wave propagation numerical model simulates accurately the propagation of regular and irregular waves in a wide range of conditions. The model behaviour has proved to be satisfactory for the usual values of the control parameters. The main exception is the breaker zone, in which the wave height is an important fraction of the water depth. However, the third order (truncation error) scheme which is now being developed, is expected to provide improved results in these cases.

- With a given $S(\omega)$, a time series $\eta(t)$ can be simulated. This signal can be used as a model input. After the run of the propagation model, the result will be another time series $\eta^*(t)$, which conveniently processed will give way to another spectral density function $S^*(\omega)$.

- With a given directional spectrum $S(\omega, \theta)$, a record with three time series ($\eta(t)$, $\eta_x(t)$, $\eta_y(t)$ for example) can be simulated, and conversely, three time series let the directional spectrum to be obtained. Up till now, the propagation model does not accept three time series as input, though it can yield these three signals as output. The efforts are now concentrated in getting the directional wave as the input of the model. In this case, a $S(\omega, \theta)$ could be the incoming one to the model, and another directional spectrum $S^*(\omega, \theta)$ could be the outgoing one.

- Numerical simulation with Boussinesq equations is an useful tool for the spectral determination and the analysis of the spectral evolution in shallow water when waves are travelling. The model has been applied succesfully to real cases. With the coupling between the Boussinesq model and the spectral techniques developed in this paper, it is possible to obtain a more compact and coherent

information on irregular wave propagation in coastal zones, bays and harbours, taking into account non-linear propagation effects.

6.- REFERENCES

- ABBOTT, M.B. and F. IONESCU (1967). "On the numerical computation of nearly-horizontal flows". J. Hyd. Res. Vol. 5

- ARCILLA, A.S. y J.L.MONSO (1985). "Modelado numérico del flujo en zonas costeras". Dirección General de Puertos y Costas, MOPU. Programa de Clima Marítimo n.7

- ARCILLA, A.S. and J.L.MONSO (1986). "Numerical modelling of Coastal Flow". Proceedings of the International Conference of Computer Techniques to Environmental Studies. Los Angeles, U.S.A.

- ARCILLA, A.S., J.L. MONSO y J.P. SIERRA (1986) "Modelo numérico no lineal de ondas de superficie libre". Dirección General de Puertos y Costas, MOPU. Programa de Clima Marítimo. n.17.

- BOUWS, E. et al. (1983). "A similarity based spectral form for limite deep water: wave growth relationships for the entire depth TMA spectral form". International Association for Hydraulic Research Conference, Moscow.

- COOLEY, J.W. and J.W. TUKEY (1965). "An alghorithm for machine calculation of complex Fourier Series". Mathematics of computation, vol.19

- HASSELMAN, K. et al. (1973). "Measurements of wind-wave growth and swell decay during the Joint North Sea Wave Project (JONSWAP)". Deust. Hydrogr. Z., Suppl. A, 8 n. 12

- PEREGRINE, D.H. (1967). "Long waves on a beach". J. Fluid Mechanics. Vol. 27

- PIERSON, W.J. and L. MOSKOWITZ (1964)."A proposed spectral form for fully developed wind seas based on the similarity theory of S.A. Kitaigorodskii". J. Geophys. Res. 69

- URSELL, F. (1953) "The long wave paradox in the theory of gravity waves". Proc. Camb. Phil. Sec. Vol. 49.